Nafta-Gaz 2023, no. 7, pp. 455–463, DOI: 10.18668/NG.2023.07.02

Viscoelastic effects under water-polymer flooding conditions of the fractured-porous reservoir

Efekty lepkosprężyste w warunkach nawadniania kolektora szczelinowo-porowego cieczą wodno-polimerową

Volodymyr G. Pogrebnyak, Volodymyr Y. Shimanskii, Andriy V. Pogrebnyak, Iryna V. Perkun

Ivano-Frankivsk National Technical University of Oil and Gas

ABSTRACT: The work is devoted to the numerical simulation of the flow of simple and viscoelastic (polymer solution) fluids through a fracture by using polymer solutions for enhanced oil recovery from a reservoir. Polymer solutions have viscoelastic properties. Therefore, when polymer solution flows through the slot, we use the well-known Maxwell's fluid model with the Jaumann derivative to evaluate deformation characteristics of the flow (stream functions, distributions of the longitudinal velocity gradient and normal stress) resulting in the manifestation of abnormal (compared with the behaviour of the ordinary fluid) effects. The case of slow flow is considered. In this case, the inertial terms can be neglected, the velocities, stresses, and stream functions can be written as the decomposition by Weisenberg number, and we can assume that the Weissenberg number is less than one. The determined regularities of viscoelastic (polymer solution) liquid behaviour with longitudinal velocity gradient and the elastic deformations effects manifested in this case have a decisive meaning in understanding the mechanism of anomalously high oil recovery capacity of a reservoir by using water-polymer flooding of the fractured-porous reservoir. Understanding the nature of the effects of elastic deformations under the conditions of water-polymer flooding of the fractured-porous reservoir enables hydrodynamic calculations of the optimal flow of the polymer solution. One of the main issues that need to be solved when developing the technology for increasing oil recovery from formations using polymer solutions is to determine the optimal flow regime in the fractured-porous reservoir. The calculation results verify the ideas obtained from the experimental solution of this problem concerning the strain-stress state of polymer macromolecules (liquid elements) during polymer flow in the inlet area of the fracture in the oil reservoir and confirm the possibility of using numerical analysis of convergent polymer flow for calculating longitudinal velocity gradients in the inlet area of the fracture and can also serve as additional substantiation of the proposed earlier mechanism for increasing oil recovery from reservoirs by using polymer solutions.

Key words: viscoelastic fluid, polymer solution, Jaumann derivative, hydrodynamic field, velocity gradient, fractured-porous reservoir.

STRESZCZENIE: Praca poświęcona jest symulacji numerycznej przepływu płynów prostych i lepkosprężystych (roztworów polimerowych) przez szczelinę z wykorzystaniem roztworów polimerowych w celu zwiększenia wydobycia ropy naftowej ze złoża. Dlatego, gdy roztwór polimeru przepływa przez szczelinę, używamy dobrze znanego modelu cieczy Maxwella z pochodną Jaumanna do oceny charakterystyk deformacji przepływu (funkcje strumienia, rozkład gradientu wzdłużnego prędkości i normalnego naprężenia), co skutkuje pojawieniem się nietypowych (w porównaniu z zachowaniem zwykłego płynu) efektów. Rozważany jest przypadek spowolnionego przepływu. W tym przypadku składowe inercyjne można pominąć, prędkości, naprężenia i funkcje strumienia można zapisać jako rozkład wg liczby Weisenberga i możemy założyć, że liczba Weissenberga jest mniejsza niż jeden. Określone prawidłowości lepkosprężystych właściwości cieczy (roztworu polimeru) z gradientem prędkości wzdłużnej, jak i przejawiające się w tym przypadku efekty odkształceń sprężystych, mają decydujące znaczenie dla zrozumienia mechanizmu anomalnie wysokiej wydajności wydobycia ropy naftowej ze złoża poprzez nawadnianie złoża szczelinowo-porowego cieczą wodno-polimerową. Zrozumienie natury efektów odkształceń sprężystych w warunkach nawadniania szczelinowo-porowatego złoża cieczą wodno-polimerową umożliwia przeprowadzenie obliczeń hydrodynamicznych optymalnego przepływu roztworu polimeru. Jednym z głównych zagadnień, które należy rozwiązać podczas opracowywania technologii zwiększania wydobycia ropy naftowej z formacji za pomocą roztworów polimerowych, jest określenie optymalnego reżimu przepływu w zbiorniku szczelinowo-porowym. Wyniki obliczeń weryfikują koncepcje uzyskane z eksperymentalnego rozwiązania tego problemu dotyczącego stanu naprężenia makrocząsteczek polimeru (elementów ciekłych) podczas przepływu polimeru w obszarze wlotowym szczeliny w zbiorniku ropy naftowej i potwierdzają możliwość zastosowania analizy

Corresponding author: V.G. Pogrebnyak, e-mail: *VGPogrebnyak@gmail.com*

Article contributed to the Editor: 27.03.2023. Approved for publication: 10.07.2023.

numerycznej zbieżnego przepływu polimeru do obliczania gradientów prędkości wzdłużnej w obszarze wlotowym szczeliny, a także mogą służyć jako dodatkowe uzasadnienie proponowanego wcześniej mechanizmu zwiększania wydobycia ropy naftowej ze złóż za pomocą roztworów polimerowych.

Słowa kluczowe: ciecz lepkosprężysta, roztwór polimeru, pochodna Jaumanna, pole hydrodynamiczne, gradient prędkości, złoże szczelinowo-porowe.

Introduction

Today, there are a lot of methods to enhance oil recovery from reservoirs, but most of them are environmentally hazardous. The most effective methods that allow extracting up to 40–45% of oil are the methods involving injection of acid, alkalis and other active chemicals into the formation (Boiko et al., 1996). Nevertheless, in the process of oil production, contamination of the environment occurs. Great damage is caused to it by chemical reagents during their injection into the reservoir or delivery to the field (Kachurin et al., 2011; Bondarenko et al., 2015).

For this reason, solving the problem of improving the environmental efficiency of oil recovery methods becomes now a relevant and urgent issue.

Among the methods of increasing oil displacement from reservoirs, polymer flooding is considered to align well with environmental standards, although its effectiveness may vary (Sheng et al., 2015). Polymer flooding is a mature enhanced-oil-recovery method with a high success rate for developing depleted oil reservoirs. Biopolymers and synthetic polymers are widely used in polymer flooding. Conventional shear rheological methods are sufficient to characterize the porous-media behaviour of viscous biopolymers. However, synthetic enhanced-oil-recovery polymers exhibit complex viscoelastic phenomena in porous and fractured-porous reservoirs (Pogrebnyak and Pisarenko, 1999; Pogrebnyak and Voloshin, 2010), which causes an additional flow resistance, higher than that expected from their shear forces. From the application point of view, it is believed that the polymer's viscoelasticity might lead to a reduced injectivity and an enhanced residual oil recovery.

Sheng et al. (2015) discussed the lessons learned from past projects and gave a brief description of the polymers' viscoelastic properties. In another publication (Wei et al., 2014), the mechanism associated with residual oil recovery by viscoelastic polymers was reviewed. Viscoelastic polymers are widely used in enhanced-oil-recovery; however, quantification of polymers' viscoelastic effect is one of the major challenges faced by the enhanced-oil-recovery researchers. Several attempts were made in this regard through the Deborah number, continuum viscoelastic models, and pore-scale studies (Azad and Trivedi, 2019).

It is obvious that one of the main issues that need to be solved during the development of the technology for increasing oil recovery from formations by using polymer solutions is to determine the optimal flow regime in the fractured-porous reservoir. Technological indicators when to use polymer solutions to increase oil recovery from the reservoir are calculated being based on the condition of satisfying the inequality (Pogrebnyak and Voloshin, 2010):

$$\dot{\varepsilon} \cdot \theta_c \leq De_{cr} \tag{1}$$

where:

θ_c – relaxation time of the polymer solution,

$\dot{\varepsilon}$ – longitudinal velocity gradient,

De_{cr} – Deborah number.

Expression (1) is the criterion for the transition of a macromolecular coil from a hydrodynamically impermeable "segmental gel", where a significant part of the segments is screened, to a flowing "segmental solution" in which all segments are already hydrodynamically interacting with the solvent. When performing the above inequality in polymer solutions (polyethylene oxide, polyacrylamide, etc.) in the flow with a longitudinal velocity gradient, dynamic supramolecular structures are formed (Brestkin, 1987, Brestkin et al., 1989; Ivanyuta et al., 1992; Pogrebnyak and Naumchuk, 1992, 1995). Expression (1) should be interpreted as the Deborah number because the inverse value of the longitudinal gradient of velocity is nothing but the time scale of the stream (Astarita and Marucci, 1978).

Thus, the calculations involve calculating the relaxation time (characteristic time) of the polymer solution and the occurring longitudinal velocity gradient, which is realized during of polymer solutions flow in the fractured-porous reservoir. According to the experimentally obtained data, the critical Deborah number for water solutions of polyethylene oxide (PEO) is 2.5 (Povkh et al., 1979; Pogrebnyak and Voloshin, 2010).

We obtained the following equation defining the characteristic relaxation time of the polymer solution (viscoelastic fluid):

$$\theta_c = \begin{cases} \theta_0 e^k & \text{at} \quad k < 1 \\ \theta_0 \dfrac{e^{k^{2/3}}}{k^{1/3}} & \text{at} \quad k > 1 \end{cases} \tag{2}$$

where: $[\eta]_0$ – characteristic viscosity, c – concentration of polymer in solution, and $[\eta]_0 \cdot c = k$.

Dependence θ_c/θ_0 on $[\eta]_0 \cdot c$ for *PEO* of two different molecular masses in the water as shown in Figure 1 (Pogrebnyak and Voloshin, 2010).

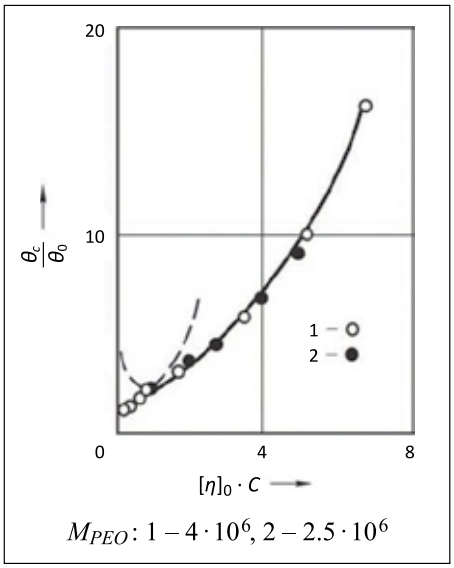

Figure 1. Profiles of θ_c/θ_0 for varying $[\eta]_0 \cdot C$ and different *PEO* concentration in solution

Rysunek 1. Profile θ_c/θ_0 dla różnych $[\eta]_0 \cdot C$ oraz różnych stężeń *PEO* w roztworze

The solid line shows the course of the dependence obtained for equation (2). We can see that the points obtained during the experiments for the corresponding concentration regions lie satisfactorily on the estimated curve.

So, substituting the known molecular characteristics of the polymer into equation (2) we can calculate the relaxation time of polymer solutions. The effect of temperature in this equation is taken into account through the temperature dependence θ_0 i k.

At the same time, research literature to our knowledge does not highlight any analytical equations for calculating a longitudinal velocity gradient in the input area of the slot or in the entry area of the round hole. To calculate the longitudinal velocity gradient of the polymer solution flow in the input area of the fractured-porous, it is necessary to analyse, taking into account its viscoelastic properties, the flow of polymer solution through the slot.

Problem Statement

Polymer solutions have viscoelastic properties (Vinogradov and Malkin, 1977; Ferri, 1983; Kristensen, 1994; Lodge, 1999). Therefore, when polymer solution flows through the slot, we can use the well-known Maxwell's fluid model (Vinogradov and Malkin, 1977; Ferri, 1983; Kristensen, 1994; Lodge, 1999) with the Jaumann derivative (Nakamura, 1987) to evaluate deformation characteristics of the flow (stream functions, distributions of the longitudinal velocity gradient and normal stress) resulting in manifestation of abnormal (compared with the behaviour of the ordinary fluid) effects (Povkh et. al., 1979; Ivanyuta et al, 1985).

We chose this model because, according to Lodge (1999), the study of non-linear, non-permanent, from the view of Lagrange, currents of viscoelastic fluids do not add any new information to those already obtained by studying homogeneous or quasi-homogeneous shear deformations. In his opinion "...the only reason for detailed calculations of different types of non-linear currents is to make sure that they are practically implemented". This Lodge's statement can be interpreted in such a way that there is no need for new rheological equations to describe convergent flows (in the input area of the slot); it is enough to use the equations of a steady Couette flow (Vinogradov and Malkin, 1977), or, at least, to determine whether they can explain the specific of polymer solution convergent flow in conditions the fractured-porous reservoir.

Algorithm for the numerical solution of the problem

To describe steady streamflow in the incompressible environments, we use the following classical equations (Astarita and Marucci, 1978; Nakamura, 1987):

- the continuity equation

$$\mathcal{V}^i_{,i} = 0 \tag{3}$$

- the Cauchy motion equation

$$\rho \mathcal{V}^k \mathcal{V}^i_{,k} = -g^{ik} P_{,k} + T^{ij}_{,k} \tag{4}$$

where: g^{ik} – metric tensor, and $T^{ij}_{,k}$ is determined by covariant differentiation T^{ij}:

$$T^{ij}_{,k} = \frac{\partial T^{ij}}{\partial x^k} + \begin{Bmatrix} i & \\ k & m \end{Bmatrix} T^{mj} + \begin{Bmatrix} i & \\ k & m \end{Bmatrix} T^{im}$$

where $\begin{Bmatrix} i & \\ k & m \end{Bmatrix}$ are the Christoffel symbols expressed by the dependence:

$$\begin{Bmatrix} i & \\ k & m \end{Bmatrix} = \frac{1}{2} g^{il} \left(\frac{\partial g_{kl}}{\partial x^m} + \frac{\partial g_{ml}}{\partial x^k} - \frac{\partial g_{km}}{\partial x^l} \right)$$

Having designated θ_c to relaxation time and η_c – to viscosity, we can write the structural rheological equation of the Maxwell's fluid model (Voytkunskiy et al., 1970):

$$T^{ij} + \theta_c \frac{D_j T^{ij}}{Dt} = 2\eta_c D^{ij} \tag{5}$$

where D_j/Dt – the Jaumann derivative described by the equation

$$\frac{D_j T^{ij}}{Dt} = \frac{\partial T^{ij}}{\partial t} + \mathcal{V}^k T^{ij}_{,k} - W^i_k T^{kj} - T^{ik} W^j_k$$

in which

$$D_{km} = \frac{1}{2}(\mathcal{V}_{k,m} + \mathcal{V}_{m,k})$$

$$W_{km} = \frac{1}{2}(\mathcal{V}_{k,m} - \mathcal{V}_{m,k})$$

Analysing the case where the incompressible fluid moves between two parallel planes and flows through the slot which length is considerably longer than width. The flow is flat and stationary. Figure 2 shows the shape of the slot of the fractured-porous reservoir and Cartesian coordinates.

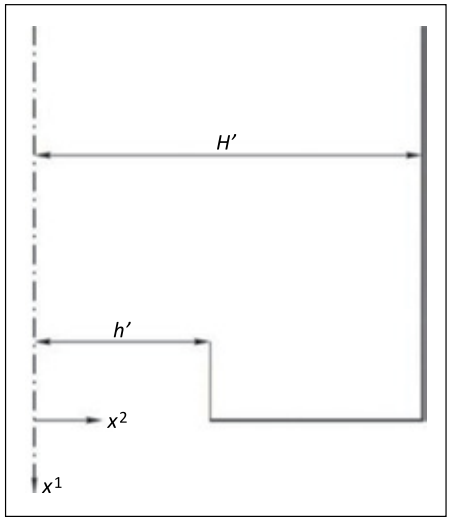

Figure 2. The shape of the slot and Cartesian coordinates
Rysunek 2. Kształt szczeliny i współrzędne kartezjańskie

The components of the metric tensor in Cartesian coordinates are:

$g_{11} = g_{22} = 1$

$g_{12} = g_{21} = 0$

The Christoffel symbols $\begin{Bmatrix} i \\ k \quad m \end{Bmatrix}$ equal zero since the components of the metric tensor g_{ik} are not coordinate-dependent. Let us express this in a dimensionless form, introducing the following quantities into equations (3), (4) and (5):

$$\begin{aligned} x_1^* &= \frac{x^1}{H'} & x_2^* &= \frac{x^2}{H'} \\ V_1^* &= \frac{\mathcal{V}^1}{\bar{u}} & V_2^* &= \frac{\mathcal{V}^2}{\bar{u}} \\ T_{11}^* &= \frac{H'}{\eta_c \bar{u}} T^{11} & T_{22}^* &= \frac{H'}{\eta_c \bar{u}} T^{22} \\ T_{12}^* &= \frac{H'}{\eta_c \bar{u}} T^{12} & T_{21}^* &= \frac{H'}{\eta_c \bar{u}} T^{21} \\ P^* &= \frac{H'}{\eta_c \bar{u}} P \end{aligned} \qquad (6)$$

where: $\bar{u}$ – average flow velocity; $2H'$ – slot width.

Considering transformations (3), (4), (5), they are reduced to:

$$\frac{\partial \mathcal{V}_1^*}{\partial x_1^*} + \frac{\partial \mathcal{V}_2^*}{\partial x_2^*} = 0 \qquad (7)$$

$$\mathrm{Re}\left(\mathcal{V}_1^* \frac{\partial \mathcal{V}_1^*}{\partial x_1^*} + \mathcal{V}_2^* \frac{\partial \mathcal{V}_1^*}{\partial x_2^*} \right) = -\frac{\partial P^*}{\partial x_1^*} + \frac{\partial T_{11}^*}{\partial x_1^*} + \frac{\partial T_{12}^*}{\partial x_2^*} \qquad (8a)$$

$$\mathrm{Re}\left(\mathcal{V}_1^* \frac{\partial \mathcal{V}_2^*}{\partial x_1^*} + \mathcal{V}_2^* \frac{\partial \mathcal{V}_2^*}{\partial x_2^*} \right) = -\frac{\partial P^*}{\partial x_2^*} + \frac{\partial T_{21}^*}{\partial x_1^*} + \frac{\partial T_{22}^*}{\partial x_2^*} \qquad (8b)$$

$$T_{11}^* + We \left\{ \begin{aligned} & \mathcal{V}_1^* \frac{\partial T_{11}^*}{\partial x_1^*} + \mathcal{V}_2^* \frac{\partial T_{11}^*}{\partial x_2^*} - \\ & -\frac{1}{2}\left(\frac{\partial \mathcal{V}_1^*}{\partial x_2^*} - \frac{\partial \mathcal{V}_2^*}{\partial x_1^*} \right)(T_{12}^* + T_{21}^*) \end{aligned} \right\} = 2\frac{\partial \mathcal{V}_1^*}{\partial x_1^*} \qquad (9a)$$

$$T_{22}^* + We \left\{ \begin{aligned} & \mathcal{V}_1^* \frac{\partial T_{22}^*}{\partial x_1^*} + \mathcal{V}_2^* \frac{\partial T_{22}^*}{\partial x_2^*} + \\ & +\frac{1}{2}\left(\frac{\partial \mathcal{V}_1^*}{\partial x_2^*} - \frac{\partial \mathcal{V}_2^*}{\partial x_1^*} \right)(T_{12}^* + T_{21}^*) \end{aligned} \right\} = 2\frac{\partial \mathcal{V}_2^*}{\partial x_2^*} \qquad (9b)$$

$$T_{12}^* + We \left\{ \begin{aligned} & \mathcal{V}_1^* \frac{\partial T_{12}^*}{\partial x_1^*} + \mathcal{V}_2^* \frac{\partial T_{12}^*}{\partial x_2^*} + \\ & +\frac{1}{2}\left(\frac{\partial \mathcal{V}_1^*}{\partial x_2^*} - \frac{\partial \mathcal{V}_2^*}{\partial x_1^*} \right)(T_{11}^* + T_{22}^*) \end{aligned} \right\} = \frac{\partial \mathcal{V}_1^*}{\partial x_2^*} + \frac{\partial \mathcal{V}_2^*}{\partial x_1^*} \qquad (9c)$$

$$T_{21}^* + We \left\{ \begin{aligned} & \mathcal{V}_1^* \frac{\partial T_{21}^*}{\partial x_1^*} + \mathcal{V}_2^* \frac{\partial T_{21}^*}{\partial x_2^*} + \\ & +\frac{1}{2}\left(\frac{\partial \mathcal{V}_1^*}{\partial x_2^*} - \frac{\partial \mathcal{V}_2^*}{\partial x_1^*} \right)(T_{11}^* + T_{22}^*) \end{aligned} \right\} = \frac{\partial \mathcal{V}_1^*}{\partial x_2^*} + \frac{\partial \mathcal{V}_2^*}{\partial x_1^*} \qquad (9d)$$

where: $\mathrm{Re} = \dfrac{\rho \bar{u} H'}{\eta_c}$ – the Reynolds number; $We = \dfrac{\theta_c \bar{u}}{H'}$ – the Weissenberg number.

If we restrict ourselves to a flow in which the inertial terms can be neglected, then the left side of equation (8) will equal zero. Applying the continuity equation (7), we introduce the stream function

$$\mathcal{V}_1^* = \frac{\partial \psi}{\partial x_2^*}, \quad \mathcal{V}_2^* = -\frac{\partial \psi}{\partial x_1^*} \qquad (10)$$

If we assume that the fluid flow at the slot input area of the oil slotted-porous reservoir has the Poiseuille velocity profile, the velocity on the surface of the solid wall (adhesion condition) equals zero, and the flow velocity is constant, the boundary conditions will take the following form:

$$x_1^* = -\infty, \ \mathcal{V}_1^* = \frac{3}{2}(1 - x_2^{*2}), \ \mathcal{V}_2^* = 0 \qquad (11a)$$

$$x_1^* = 0, \ 0 \le x_2^* \le h^*, \ \mathcal{V}_1^* = \mathcal{V}_0^*, \ \mathcal{V}_2^* = 0 \qquad (11b)$$

$$x_1^* = 0, \ h^* \le x_2^* \le 1, \ \mathcal{V}_1^* = \mathcal{V}_2^* = 0 \qquad (11c)$$

$$x_2^* = 0, \ \frac{\partial \mathcal{V}_1^*}{\partial x_2^*} = \mathcal{V}_2^* = 0 \qquad (11d)$$

$$x_2^* = 1,\ \mathcal{V}_1^* = \mathcal{V}_2^* = 0 \tag{11e}$$

where: $\mathcal{V}_0^*$ = const, determined by the expendable velocity; h^* – dimensionless value, equals h'/H'; $2H'$ – slot width.

It is necessary to solve equations (7), (8), and (9) to determine the flow and stress fields, according to the boundary conditions (11). It is not possible to solve these equations in a general form; therefore, we restrict ourselves to slow flows. In this case, we can not only neglect the inertial terms but also assume that the Weisenberg number is less than one.

Let's recall that the Weissenberg number characterizes the rate of the viscoelastic properties of the fluid in a shear flow. In the case under consideration, we have a complex flow with both shear and longitudinal velocity gradients. As the velocity of the outflow through the slot increases, as proven in (Pogrebnyak et al., 2017), the proportion of the longitudinal (stretching) flow increases, and the shear decreases. Therefore, it is more appropriate, instead of the Weissenberg number, to use a Deborah number, which characterizes the rate of viscoelastic properties in a stretching flow (Astarita and Marucci, 1978).

Nevertheless, for stationary flows, the ratio is $De/We = \mathrm{Re}^{0,75}$ (Hintse, 1963; Astarita and Marucci, 1978), which means that both criteria, *We* and *De*, are interconnected within geometrically similar flows.

Therefore, for restrictions, imposed on this flow, we can write the velocities, stress, and stream functions as the decomposition by number *We*:

$$\begin{aligned}
\mathcal{V}_i^* &= \mathcal{V}_i^{(0)} + We\,\mathcal{V}_i^{(1)} + We^2\mathcal{V}_i^{(2)} + \ldots \\
P^* &= P^{(0)} + We\,P^{(1)} + We^2P^{(2)} + \ldots \\
T_{ij}^* &= T_{ij}^{(0)} + We\,T_{ij}^{(1)} + We^2T_{ij}^{(2)} + \ldots \\
\psi^* &= \psi^{(0)} + We\,\psi^{(1)} + We^2\psi^{(2)} + \ldots
\end{aligned} \tag{12}$$

Substituting (12) into equations (7), (8), (9), and the boundary conditions (11), we will put the equation in order with respect to the Weissenberg number. Now we can write down the terms of equations that do not include the Weissenberg number:

$$\frac{\partial \mathcal{V}_1^{(0)}}{\partial x_1^*} + \frac{\partial \mathcal{V}_2^{(0)}}{\partial x_2^*} = 0 \tag{13a}$$

$$\frac{\partial T_{11}^{(0)}}{\partial x_1^*} + \frac{\partial T_{12}^{(0)}}{\partial x_2^*} = \frac{\partial P^{(0)}}{\partial x_1^*} \tag{13b}$$

$$\frac{\partial T_{21}^{(0)}}{\partial x_1^*} + \frac{\partial T_{22}^{(0)}}{\partial x_2^*} = \frac{\partial P^{(0)}}{\partial x_2^*} \tag{13c}$$

$$T_{11}^{(0)} = 2\frac{\partial \mathcal{V}_1^{(0)}}{\partial x_1^*},\ T_{22}^{(0)} = 2\frac{\partial \mathcal{V}_2^{(0)}}{\partial x_2^*} \tag{13d}$$

$$T_{12}^{(0)} = \frac{\partial \mathcal{V}_1^{(0)}}{\partial x_1^*} + \frac{\partial \mathcal{V}_2^{(0)}}{\partial x_1^*} \tag{13e}$$

$$T_{21}^{(0)} = \frac{\partial \mathcal{V}_1^{(0)}}{\partial x_1^*} + \frac{\partial \mathcal{V}_2^{(0)}}{\partial x_1^*} \tag{13f}$$

$$\mathcal{V}_1^{(0)} = \frac{\partial \psi^{(0)}}{\partial x_2^*},\ \mathcal{V}_2^{(0)} = -\frac{\partial \psi^{(0)}}{\partial x_1^*} \tag{13g}$$

Boundary conditions:

$$\begin{aligned}
&x_1^* = -\infty,\ \mathcal{V}_1^{(0)} = \frac{3}{2}(1 - x_2^{*2}),\ \mathcal{V}_2^{(0)} = 0 \\
&x_1^* = 0,\ 0 \le x_2^* \le h^*,\ \mathcal{V}_1^{(0)} = \mathcal{V}_0^*,\ \mathcal{V}_2^{(0)} = 0,\ x_2^* = 0,\ \frac{\partial \mathcal{V}_1^{(0)}}{\partial x_2^*} = \mathcal{V}_2^{(0)} = 0 \\
&x_1^* = 0,\ h^* \le x_2^* \le 1,\ \mathcal{V}_1^{(0)} = \mathcal{V}_2^{(0)} = 0,\ x_2^* = 1,\ \mathcal{V}_1^{(0)} = \mathcal{V}_2^{(0)} = 0
\end{aligned} \tag{14}$$

Considering equation (13), by expressing $\frac{\partial P^{(0)}}{\partial x_1^*}, \frac{\partial P^{(0)}}{\partial x_2^*}$ through $\Psi^{(0)}$ and its derivatives and excluding $P^{(0)}$, we obtain:

$$\left(\frac{\partial^2}{\partial x_1^{*2}} + \frac{\partial^2}{\partial x_2^{*2}}\right)\psi^{(0)} = 0 \tag{15}$$

For boundary conditions (14) the solution of the equation (15) describes the flow of the ordinary fluid.

$$\psi^{(0)} = \psi^{(0)}(x_1^*, x_2^*,)$$

By substituting equation (12) into equation (9) and grouping the terms with the Weissenberg number in the first power, we obtain:

$$\begin{aligned}
T_{11}^{(1)} = {} & \frac{1}{2}\left(\frac{\partial \mathcal{V}_1^{(0)}}{\partial x_2^*} + \frac{\partial \mathcal{V}_2^{(0)}}{\partial x_1^*}\right)(T_{12}^{(0)} + T_{21}^{(0)}) + \\
& + 2\frac{\partial \mathcal{V}_1^{(1)}}{\partial x_1^*} - \mathcal{V}_1^{(0)}\frac{\partial T_{11}^{(0)}}{\partial x_1^*} - \mathcal{V}_2^{(0)}\frac{\partial T_{11}^{(0)}}{\partial x_2^*}
\end{aligned} \tag{16a}$$

$$\begin{aligned}
T_{22}^{(1)} = {} & 2\frac{\partial \mathcal{V}_2^{(1)}}{\partial x_2^*} - \frac{1}{2}\left(\frac{\partial \mathcal{V}_1^{(0)}}{\partial x_2^*} - \frac{\partial \mathcal{V}_2^{(0)}}{\partial x_1^*}\right)(T_{12}^{(0)} + T_{21}^{(0)}) - \\
& - \mathcal{V}_1^{(0)}\frac{\partial T_{22}^{(0)}}{\partial x_1^*} - \mathcal{V}_2^{(0)}\frac{\partial T_{22}^{(0)}}{\partial x_2^*}
\end{aligned} \tag{16b}$$

$$\begin{aligned}
T_{12}^{(1)} = {} & \frac{\partial \mathcal{V}_1^{(1)}}{\partial x_2^*} + \frac{\partial \mathcal{V}_2^{(1)}}{\partial x_1^*} - \frac{1}{2}\left(\frac{\partial \mathcal{V}_1^{(0)}}{\partial x_2^*} - \frac{\partial \mathcal{V}_2^{(0)}}{\partial x_1^*}\right)(T_{11}^{(0)} - T_{22}^{(0)}) - \\
& - \mathcal{V}_1^{(0)}\frac{\partial T_{12}^{(0)}}{\partial x_1^*} - \mathcal{V}_2^{(0)}\frac{\partial T_{12}^{(0)}}{\partial x_2^*}
\end{aligned} \tag{16c}$$

$$\begin{aligned}
T_{21}^{(1)} = {} & \frac{\partial \mathcal{V}_1^{(1)}}{\partial x_2^*} + \frac{\partial \mathcal{V}_2^{(1)}}{\partial x_1^*} - \frac{1}{2}\left(\frac{\partial \mathcal{V}_1^{(0)}}{\partial x_2^*} - \frac{\partial \mathcal{V}_2^{(0)}}{\partial x_1^*}\right)(T_{11}^{(0)} - T_{22}^{(0)}) - \\
& - \mathcal{V}_1^{(0)}\frac{\partial T_{21}^{(0)}}{\partial x_1^*} - \mathcal{V}_2^{(0)}\frac{\partial T_{21}^{(0)}}{\partial x_2^*}
\end{aligned} \tag{16d}$$

where: $\mathcal{V}_i^{(0)}, T_{ij}^{(0)}$ – the velocity and stress components of the terms of equations having the Weissenberg number in a zero power, respectively; they are known.

In the similar way, converting the continuity equation, the equation of motion and the boundary conditions, we obtain:

$$\frac{\partial \mathcal{V}_1^{(1)}}{\partial x_1^*} + \frac{\partial \mathcal{V}_2^{(1)}}{\partial x_2^*} = 0 \tag{17a}$$

$$\frac{\partial T_{11}^{(1)}}{\partial x_1^*} + \frac{\partial T_{12}^{(1)}}{\partial x_2^*} = \frac{\partial P^{(1)}}{\partial x_1^*} \tag{17b}$$

$$\frac{\partial T_{21}^{(1)}}{\partial x_1^*} + \frac{\partial T_{22}^{(1)}}{\partial x_2^*} = \frac{\partial P^{(1)}}{\partial x_2^*} \tag{17c}$$

Boundary conditions:

$$\begin{aligned} x_1^* &= -\infty \quad \mathcal{V}_1^{(1)} = \mathcal{V}_2^{(1)} = 0 \\ x_1^* &= 0 \quad \mathcal{V}_1^{(1)} = \mathcal{V}_2^{(1)} = 0 \\ x_2^* &= 1 \quad \mathcal{V}_1^{(1)} = \mathcal{V}_2^{(1)} = 0 \\ x_2^* &= 0 \quad \mathcal{V}_1^{(1)} = \mathcal{V}_2^{(1)} = 0 \end{aligned} \tag{18}$$

The stream function (10) takes the following form:

$$\mathcal{V}_1^{(1)} = \frac{\partial \psi^{(1)}}{\partial x_2^*} \quad \mathcal{V}_2^{(1)} = -\frac{\partial \psi^{(1)}}{\partial x_1^*} \tag{19}$$

Considering (19) and excluding equation (17), we obtain this equation:

$$\left(\frac{\partial^2}{\partial x_1^{*2}} + \frac{\partial^2}{\partial x_2^{*2}} + \right)^2 \psi^{(1)} = 0 \tag{20}$$

The solution of equation (20) with boundary conditions (18) has the form $\Psi^{(1)} = 0$, consequently, the terms of the equation with the Weissenberg number in the first power do not affect the velocity distribution. However, as we can see from equation (16), stress $T_{11}^{(1)}$, $T_{22}^{(1)}$, $T_{12}^{(1)}$, $T_{21}^{(1)}$, prove the influence of the elasticity of the terms of the equation with the Weissenberg number in the first power. By substituting equation (12) into equation (19), taking into account that $\mathcal{V}_1^{(1)} = \mathcal{V}_2^{(1)} = 0$, and grouping the terms containing the Weissenberg number in the second power, we obtain:

$$T_{11}^{(2)} = 2\frac{\partial \mathcal{V}_1^{(2)}}{\partial x_1^*} + \frac{1}{2}\left(\frac{\partial \mathcal{V}_1^{(0)}}{\partial x_2^*} - \frac{\partial \mathcal{V}_2^{(0)}}{\partial x_1^*} \right)(T_{12}^{(1)} + T_{21}^{(1)}) - \\ -\mathcal{V}_1^{(0)} \frac{\partial T_{11}^{(1)}}{\partial x_1^*} - \mathcal{V}_2^{(0)} \frac{\partial T_{11}^{(1)}}{\partial x_2^*} \tag{21a}$$

$$T_{22}^{(2)} = 2\frac{\partial \mathcal{V}_2^{(2)}}{\partial x_2^*} - \frac{1}{2}\left(\frac{\partial \mathcal{V}_1^{(0)}}{\partial x_2^*} - \frac{\partial \mathcal{V}_2^{(0)}}{\partial x_1^*} \right)(T_{12}^{(1)} + T_{21}^{(1)}) - \\ -\mathcal{V}_1^{(0)} \frac{\partial T_{22}^{(1)}}{\partial x_1^*} - \mathcal{V}_2^{(0)} \frac{\partial T_{22}^{(1)}}{\partial x_2^*} \tag{21b}$$

$$T_{12}^{(2)} = \frac{\partial \mathcal{V}_1^{(2)}}{\partial x_2^*} + \frac{\partial \mathcal{V}_2^{(2)}}{\partial x_1^*} - \frac{1}{2}\left(\frac{\partial \mathcal{V}_1^{(0)}}{\partial x_2^*} - \frac{\partial \mathcal{V}_2^{(0)}}{\partial x_1^*} \right)(T_{11}^{(1)} - T_{22}^{(1)}) - \\ -\mathcal{V}_1^{(0)} \frac{\partial T_{12}^{(1)}}{\partial x_1^*} - \mathcal{V}_2^{(0)} \frac{\partial T_{12}^{(1)}}{\partial x_2^*} \tag{21c}$$

$$T_{21}^{(2)} = \frac{\partial \mathcal{V}_1^{(2)}}{\partial x_2^*} + \frac{\partial \mathcal{V}_2^{(2)}}{\partial x_1^*} - \frac{1}{2}\left(\frac{\partial \mathcal{V}_1^{(0)}}{\partial x_2^*} - \frac{\partial \mathcal{V}_2^{(0)}}{\partial x_1^*} \right)(T_{11}^{(1)} - T_{22}^{(1)}) - \\ -\mathcal{V}_1^{(0)} \frac{\partial T_{21}^{(1)}}{\partial x_1^*} - \mathcal{V}_2^{(0)} \frac{\partial T_{21}^{(1)}}{\partial x_2^*} \tag{21d}$$

Once index (1) was substituted by (2) in equations (17), (18) and (19), the continuity equations, the equations of motion, the boundary conditions and the stream function took the same form.

Therefore, excluding $P^{(2)}$, we will get:

$$\left(\frac{\partial^2}{\partial x_1^{*2}} + \frac{\partial^2}{\partial x_2^{*2}} \right)^2 \psi^{(2)} = \frac{\partial^2 \mathcal{V}_1^{(0)}}{\partial x_2^* \partial x_1^*}\left(\frac{\partial A}{\partial x_1^*} + \frac{\partial A}{\partial x_2^*} \right) + \\ + \frac{\partial \mathcal{V}_1^{(0)}}{\partial x_2^*}\left(\frac{\partial^2 A}{\partial x_1^{*2}} + 2\frac{\partial^2 T_{12}^{(1)}}{\partial x_2^* \partial x_1^*} \right) + \frac{\partial \mathcal{V}_2^{(0)}}{\partial x_1^*}\left(\frac{\partial^2 A}{\partial x_2^{*2}} - 2\frac{\partial^2 T_{12}^{(1)}}{\partial x_1^* \partial x_2^*} \right) - \\ -C\frac{\partial^2 B}{\partial x_1^* \partial x_2^*} - \frac{B}{2}\left(2\frac{\partial^2 C}{\partial x_1^* \partial x_2^*} - \frac{\partial^2 A}{\partial x_2^{*2}} + \frac{\partial^2 A}{\partial x_1^{*2}} \right) - \\ -\frac{\partial B}{\partial x_1^*}\left(\frac{\partial C}{\partial x_2^*} + \frac{\partial A}{\partial x_1^*} \right) + \frac{\partial B}{\partial x_2^*}\left(\frac{\partial A}{\partial x_2^*} - \frac{\partial C}{\partial x_1^*} \right) + \frac{\partial^2 \mathcal{V}_1^{(0)}}{\partial x_2^{*2}} \cdot \frac{\partial T_{12}^{(1)}}{\partial x_1^*} + \\ + \frac{\partial^2 \mathcal{V}_2^{(0)}}{\partial x_2^{*2}} \cdot \frac{\partial T_{12}^{(1)}}{\partial x_2^*} - \frac{\partial^2 \mathcal{V}_1^{(0)}}{\partial x_1^{*2}} \cdot \frac{\partial T_{12}^{(1)}}{\partial x_1^*} - \frac{\partial^2 \mathcal{V}_2^{(0)}}{\partial x_1^{*2}} \cdot \frac{\partial T_{21}^{(1)}}{\partial x_2^*} + \\ +2\frac{\partial \mathcal{V}_2^{(0)}}{\partial x_2^{*2}}\left(\frac{\partial^2 T_{12}^{(1)}}{\partial x_2^{*2}} + \frac{\partial^2 T_{12}^{(1)}}{\partial x_1^{*2}} \right) + \frac{A}{2}\left(\frac{\partial^2 B}{\partial x_2^{*2}} - \frac{\partial^2 B}{\partial x_1^{*2}} \right) + \\ +\mathcal{V}_1^{(0)}\left(\frac{\partial^3 T_{12}^{(1)}}{\partial x_2^{*2} \partial x_1^*} - \frac{\partial^3 T_{12}^{(1)}}{\partial x_1^{*3}} + \frac{\partial^3 A}{\partial x_1^{*2} \partial x_2^*} \right) + \\ +\mathcal{V}_2^{(0)}\left(\frac{\partial^3 T_{12}^{(1)}}{\partial x_2^{*3}} - \frac{\partial^3 T_{12}^{(1)}}{\partial x_2^{*2} \partial x_2^*} + \frac{\partial^3 A}{\partial x_2^{*2} \partial x_1^*} \right) \tag{22}$$

where:

$$A = T_{11}^{(1)} - T_{22}^{(1)}, \quad B = \frac{\partial \mathcal{V}_1^{(0)}}{\partial x_2^*} - \frac{\partial \mathcal{V}_2^{(0)}}{\partial x_1^*}, \quad C = T_{12}^{(1)} + T_{21}^{(1)}.$$

Since the right-hand side of equation (22) is known, solving equation (22), which includes boundary conditions, will give the terms of the equation with the Weissenberg number in the second power. These terms characterize the distribution of velocities and stresses.

Results and Discussion

Figures 3 and 4 visualise the stream function when ordinary ($We = 0$) and Maxwell ($We = 0.1$) fluids flow through the slot. Obviously, as the channel compression ratio decreases, the stream function experiences an increasing impact at the inlet slot. When the Maxwell fluid flows through a simulated slotted chamber, the circulation zone (Figure 3b) arises, which extends from the right corner of the channel to the

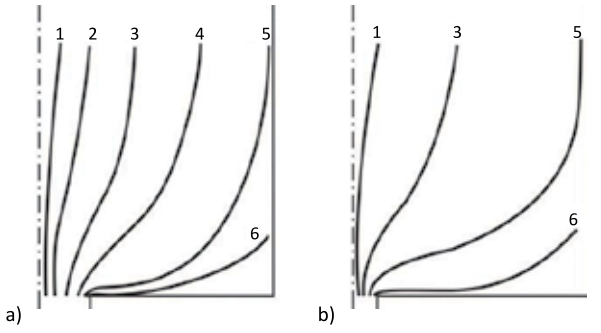

We = 0, Ψ:
1 – 0.125, 2 – 0.375, 3 – 0.625, 4 – 0.875, 5 – 0.9715, 6 – 1.0;
a) h'/H' – 0.2; b) h'/H' – 0.07

Figure 3. The stream function, when flowing through the slot of the Newtonian fluid

Rysunek 3. Funkcja strumienia podczas przepływu przez szczelinę płynu newtonowskiego

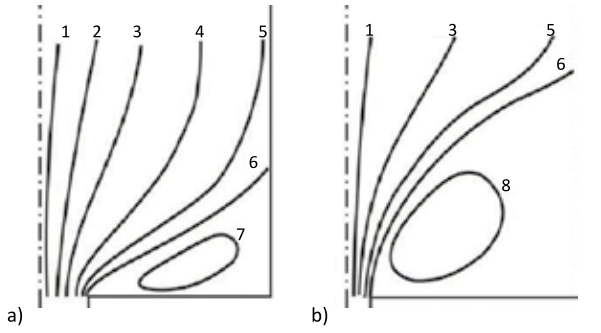

We = 0.1, Ψ:
1 – 0.125, 2 – 0.375, 3 – 0.625, 4 – 0.875, 5 – 0.9715, 6 – 1.0,
7 – 1.01, 8 – 1.1;
a) h'/H' – 0.2; b) h'/H' – 0.07

Figure 4. The stream function when flowing through the slot of the Newtonian fluid

Rysunek 4. Funkcja strumienia podczas przepływu przez szczelinę płynu newtonowskiego

slot and occupies a triangular area. The flow lines form the inlet flow. Consequently, a decrease in the channel compression ratio (as well as an increase in *We*) results in the input flooded jet.

Figure 5 shows the distribution of the dimensionless longitudinal velocity gradient along the flow axis when ordinary (curves 1 and 2) and Maxwell (curve 3) fluids flow into the slot. We can see that the maximum value of the velocity gradient in the flow of an ordinary fluid is reached at the distance $3h'$ and h' (x_1* = 1.5) from the slot for the compression ratios of 0.2 and 0.07, respectively. The flowing fluid acquires the viscoelastic properties what shifts the maximum on the curve $\dot{\varepsilon}^* = f(x_1^*)$ to the region of large x^1 and decreases the value of $\dot{\varepsilon}^*_{max}$.

A comparison of the experimental data obtained in (Ivanyuta et al., 1985, 1992; Pogrebnyak et al., 2019, 2022) with the

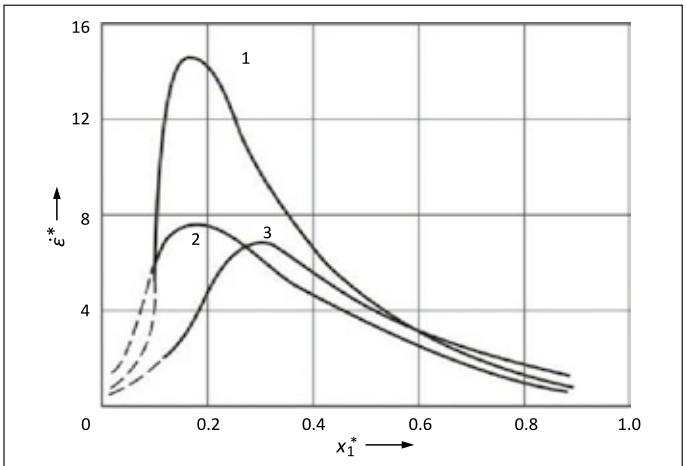

1: h'/H' = 0.07, *We* = 0;
2: h'/H' = 0.20, *We* = 0;
3: h'/H' = 0.20, *We* = 0.1

Figure 5. The distribution of the dimensionless longitudinal velocity gradient along the axis of the fluid flowing into the slot

Rysunek 5. Rozkład bezwymiarowego gradientu wzdłużnego prędkości wzdłuż osi płynu wpływającego do szczeliny

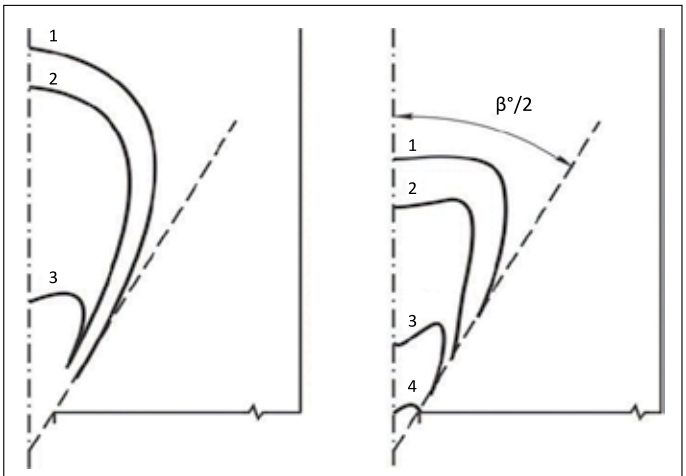

a) *We* = 0.1, h'/H' = 0.07; T^*: 1 – 5, 2 – 7, 3 – 45;
b) Δ*n*: 1 – 10^{-4}, 2 – $7 \cdot 10^{-4}$, 3 – $15 \cdot 10^{-4}$, 4 – $62 \cdot 10^{-4}$

Figure 6. The distribution of dimensionless normal stresses (a) and isochromes (b) in the input area of a slot

Rysunek 6. Rozkład bezwymiarowych naprężeń normalnych (a) i izochrom (b) w obszarze wlotowym szczeliny

results of the numerical simulations shows that the simulated flow lines and the distribution of the velocity gradient correspond to the experimentally obtained results.

The distribution of dimensionless normal stress for the channel compression ratio of 0.07 and the Weissenberg number 0.1 is shown in Figure 6. The results properly visualise the experimental data on the distribution of isochromes in the input area of the slot (Figure 6b and (Brestkin et al., 1988)). As in the polystyrene-bromoform system under consideration both the polymer and the solvent had the same refractive indices,

the obtained lines of equal birefringence value (isochromes) inside the input flooded jet are proportional to the first difference of normal stresses.

The obtained results indicate that the numerical method of the convergent flow analysis of Maxwell's highly viscoelastic fluid can be used to calculate the longitudinal velocity gradients realized in the inlet area of cracks during the flow of polymer solutions in the fractured-porous reservoirs. It should be noted, however, that in the general case it is necessary to take into account the influence of the entry angle into the slot, which can be done by considering the problem in rectilinear inclined or curvilinear coordinates. At the same time, the analysis of the viscoelastic fluid flow in the fractured-porous reservoir is sharply complicated.

Conclusions

1. The conducted analysis of the viscoelastic fluid leakage through the fracture has defining value, first of all, for confirming the interpretation of experimental data proposed by Ivanyuta et al. (1985, 1992), Pogrebnyak et al. (2019, 2022), which characterize special aspects of the convergent flow of aqueous polymer solutions in the inlet area of the hole or fracture.
2. The calculation results verify the ideas obtained from the experimental solution of this problem concerning the strain-stress state of polymer macromolecules (liquid elements) during polymer flow in the inlet area of the fracture in the oil reservoir and confirm the possibility of using numerical analysis of convergent polymer flow for calculating longitudinal velocity gradients in the inlet area of the fracture, and can also serve as additional substantiation of the proposed by Pogrebnyak and Voloshin (2010), Pogrebnyak and Pisarenko (1999) mechanism for increasing oil recovery from reservoirs by using polymer solutions.

References

Astarita J., Marucci J., 1978. Osnovyi gidromehaniki nenyutonovskih zhidkostey. *Monografiy, Wydawnictwa Mir, Moscow*, 1–309.

Azad M.S., Trivedi J.J., 2019. Quantification of the Viscoelastic Effects During Polymer Flooding: a Critical Review. *SPA Journal*, 24(06): 2731–2757. DOI: 10.2118/195687-PA.

Boiko V.S., Kondrat R.M., Yaremiichuk Z.S.,1996. Dovidnyk z naftohazovoi spravy. *Wydawnictwa Svit, L'viv*, 1–620.

Bondarenko A.V., Kudryashova D.A., 2015. The application of hydrodynamic modeling for predictive effectiveness assessment of polymer flooding technology on Moskudinskoye field. *Oil Industry*, 10: 102–105.

Brestkin Yu.V., 1987. Dynamic coil–extended chain phase transition in the longitudinal field. *Acta Polymerica*, 38(8): 470–477. DOI: 10.1002/actp.1987.010380803.

Brestkin Yu.V., Ahranova S.F., D'iakova N.E., Pogrebnyak V.G., Tverdokhleb S.V., 1989. Birefringence effects of polymer-solutions in hydrodynamic fields. *Vysokomolekulyarnye Soedineniya, Seriya B*, 31(11): 844–846.

Brestkin Yu.V., Amribakhshov A.A., Kholmuminov A.A., Frenkel S.Y., 1988. Razvorachivanie makromolekul pri shodyaschemsya techenii. *Izv. AN UzSSR, Seriya phiz.-mat. nauk.*, 6: 80–84.

Ferri J., 1983. Vyazkouprugie svoystva polimerov. *Monografiy, Wydawnictwa, Inostr. Lit., Moscow*, 1–535.

Hintse I.O., 1963. Turbulentnost. Mehanizm i teoriya. *Monografiy, Wydawnictwa, Phiz.-mat. Izdat., Moscow*, 1–680.

Ivanyuta Yu.F., Naumchuk N.V., Pogrebnyak V.G., Tverdokhleb S.V., Frenkel S.Ya., 1985. Flow structure of aqueous solutions of polyethylene oxide in the inlet region of short capillaries. *Journal of Engineering Physics*, 49(4): 1192–1197. DOI: 10.1007/BF00871917.

Ivanyuta Yu.F., Pogrebnyak V.G., Frenkel S.Ya., 1992. Structure of the hydrodynamic field and strain behavior of flexible macromolecules in convergent flow. *Vysokomolekulyarnye Soedineniya, Seriya A*, 34(3): 133–138.

Kachurin A., Sattarov R., Ayupova D., Gabdullina A., 2011. Improvement of the technology of strata oil recovery enhancement using Soft Pusher Polyacrylamide in the fields of LUKOIL –Western Siberia. *Oil Industry*, 8: 126–128.

Kristensen R., 1994. Vvedenie v teoriyu vyazkouprugosti. *Monografiy, Wydawnictwa, Mir, Moscow*, 1–338.

Lodge A.S., 1999. Elastichnyie zhidkosti. Vvedenie v reologiyu konechnodeformiruemyih polimerov. *Monografiy, Wydawnictwa, Nauka, Moscow*, 1–463.

Nakamura K., 1987. Medlennoe istechenie vyazkouprugoy zhidkosti po konicheskomu kanalu. *Senk'i kikay gakkay si.*, 31(8): 49–64.

Pogrebnyak A., Chudyk I., Pogrebnyak V., Perkun I., 2019. Coil--uncoiled chain transition of polyethylene oxide solutions under convergent flow. *Chemistry and Chemical Technology*, 13(4): 465–470. DOI: 10.23939/chcht13.04.465.

Pogrebnyak V.G., Chudyk I.I., Pogrebnyak A.V., Perkun I.V., 2022. Perforation of oil and gas wells by a high-velocity jet of polymer solution. *Nafta-Gaz*, 78(1): 3–13. DOI: 10.18668/NG.2022.01.01.

Pogrebnyak V.G., Naumchuk N.V., 1992. Dynamic structurization in solutions of hydrodynamically active polymers. *Journal of Engineering Physics and Thermophysics*, 63(2): 763–765. DOI: 10.1007/BF00861695.

Pogrebnyak V.G., Naumchuk N.V., 1995. On the hydrodynamic activity of polymers in high-velocity flows. *Inzhenerno-Fizicheskii Zhurnal*, 68(1): 146–148.

Pogrebnyak A.V., Perkun I.V., Pogrebnyak V.G., 2017. Degradation of Polymer Solutions in a Hydrodynamic Field with a Longitudinal Velocity Gradient. *Journal of Engineering Physics and Thermophysics*, 90(5): 1219–1224. DOI: 10.1007/s10891-017-1677-8.

Pogrebnyak V.G., Pisarenko A.A., 1999. Deformation effects in case of a flow with stretching of polymer solutions. Banerjee S., Eaton J.K. (ed.), Turbulence and Shear flow phenomena. *1 First International Symposium Santa Barbara, California*, 1345–1350.

Pogrebnyak V.G., Voloshin V.S., 2010. Ecological Technology of Creating Waterproof Screens. *Monograph, Publisher Knowledge, Donets*, 1–482.

Povkh I. L., Pogrebnyak V. G., Toryanik A. I., 1979. Relation between molecular structure of polyethyleneoxide and drag reduction. *Journal of Engineering Physics*, 37(4): 1131–1136.

Sheng J.J., Leonhardt B., Azri N., 2015. Status of Polymer-Flooding Technology. *Journal of Canadian Petroleum Technology*, 54 (2): 116–126. DOI: 10.2118/174541-PA.

Vinogradov G.V., Malkin A.Ya., 1977. Reologiya polimerov. *Monografiy, Wydawnictwa Khimiya, Moscow*, 1–440.

Voytkunskiy Ya.I., Amfilohiev V.V., Pavlovskiy V.A., 1970. *Sb. nauch. tr. Leningr. korablestr. ins-t*, 69: 19–25.

Wei B., Romero-Zerón L.R., Rodrigue D., 2014. Oil displacement mechanisms of viscoelastic polymers in enhanced oil recovery: a review. *Journal of Petroleum Exploration and Production Technology*, 4 (2): 113–121. DOI: 10.1007/s13202-013-0087-5.

Prof. Volodymyr G. POGREBNYAK, Ph.D., D.Sc.
Head of the Department of Technogenic, Environmental Technology and Labor Safety
Ivano-Frankivsk National Technical University of Oil and Gas
15 Karpatska St., Ivano-Frankivsk, 76019, Ukraine
E-mail: *VGPogrebnyak@gmail.com*

Andriy V. POGREBNYAK, Ph.D., D.Sc.
Chief Researcher
Ivano-Frankivsk National Technical University of Oil and Gas
15 Karpatska St., Ivano-Frankivsk, 76019, Ukraine
E-mail: *pogrebnyak.av@gmail.com*

Volodymyr Y. SHIMANSKII, M.Sc.
Associate Professor at the Department of Technogenic Environmental Technology and Labor Safety
Ivano-Frankivsk National Technical University of Oil and Gas
15 Karpatska St., Ivano-Frankivsk, 76019, Ukraine
E-mail: *shuman.vova@gmail.com*

Iryna V. PERKUN, Ph.D.
Associate Professor at the Department of Technogenic, Environmental Technology and Labor Safety
Ivano-Frankivsk National Technical University of Oil and Gas
15 Karpatska St., Ivano-Frankivsk, 76019, Ukraine
E-mail: *perkuniv@gmail.com*